Thermally Stable Intermolecular Proton Bonds in Polyaromatic Aldehyde Crystals

ARTICLE *in* CHEMISTRY - AN ASIAN JOURNAL · AUGUST 2011

Impact Factor: 4.59 · DOI: 10.1002/asia.201100130 · Source: PubMed

7 AUTHORS, INCLUDING:

Nongmaithem Jiten Singh
Pohang University of Science and Technology
54 PUBLICATIONS **2,803** CITATIONS
SEE PROFILE

Kwang-Sun Kim
Korea University of Technology and Educat…
554 PUBLICATIONS **30,527** CITATIONS
SEE PROFILE

CHEMISTRY
AN ASIAN JOURNAL

DOI: 10.1002/asia.201100130

VIP

Thermally Stable Intermolecular Proton Bonds in Polyaromatic Aldehyde Crystals

Sung Woo Heo,[b] In-Chul Hwang,[a] Young Chun,[a] Jung Woo Lee,[a] N. Jiten Singh,[a] Seung Bin Kim,[b] and Kwang S. Kim*[a]

Dedicated to Professor Eun Lee on the occasion of his retirement and 65th birthday

Abstract: We have synthesized self-assembled red-colored proton complexes of the aldehyde derivatives of polyaromatic hydrocarbon with strong intermolecular hydrogen bonding. These intermolecularly proton-bonded polyaromatic aldehydes formed as 1-pyrenecarbaldehyde (Py-CHO) reacted with $HAuCl_4$ to produce $[(Py\text{-}CHO)_2H][AuCl_4]$ under dry conditions. The formation of $[(Py\text{-}CHO)_2H][AuCl_4]$ was confirmed by single-crystal structure determination and IR spectral analysis at various temperatures. The compounds are distinctively hydrophobic in nature and are soluble only in a few organic polar solvents. The proton bonds are clearly observed from both the electron density in X-ray analysis and the characteristic IR frequency signature. The proton complex units have an O–H^+–O distance of the typical Zundel-like cationic hydrogen bond (in which two O atoms share a proton-like H in the midpoint of the short O–O distance of ≈2.4 Å). The proton bonds are thermally stable, even over 100 °C, because the complexes are stabilized in layered structures with π–π intermolecular interactions of the polyaromatic hydrocarbon ligands. The IR signatures at around 900, 1200, and 1700 cm^{-1} for the Zundel-like proton bond are clearly characterized.

Keywords: crystal engineering · density functional calculations · hydrogen bonds · IR spectroscopy · proton bonds

Introduction

Diverse hydrogen-bonding types[1] can be classified in terms of strength from weak to strong.[2] Hydrogen bonding has played a crucial role in molecular recognition, sensing, association/dissociation, and assembly.[3] The neutral –O–H···O= type bond is ubiquitous and regarded as normal hydrogen bonding, such as that observed in water.[4] The anionic hydrogen-bond type of –O···H···O$^-$– [–O–H···O$^-$–; –O$^-$···H^+ ···O$^-$–; (–O–H–O–)$^-$] is associated with oxyanions, which play an important role in lowering the transition barrier in various enzymatic mechanism.[5] Strong cationic hydrogen bonds are also known, such as those found in protonated water clusters.[6] Some of the proton complexes were crystallographically characterized.[7,8] Recently, a series of proton-bonded simple organic dimers (such as MeO–H^+–OMe) generated in the gas phase were investigated with IR spectroscopy.[9] The assignment of the characteristic vibrational signals of the O–H^+–O moiety in the gas phase requires high levels of sophisticated instrumentation.[6,9]

In the case of neutral hydrogen bonds, the interoxygen distance is 2.7–2.9 Å. For hydrogen-bonded relay systems (composed of consecutive hydrogen bonds), the interoxygen distances become shorter and stronger (down to ≈2.64 Å).[10,11] In anionic hydrogen-bonding systems, the interoxygen distance of the anionic (–O–H–O–)$^-$ moiety is generally 2.4–2.6 Å, such as in $H_3O_2^-$.[12] In cationic hydrogen bonds, the hydrogen-bonding distance of the cationic (–O–H–O–)$^+$ moiety is 2.4–2.5 Å, such as in $H_5O_2^+$.[13] The

[a] Prof. I.-C. Hwang,[+] Y. Chun, J. W. Lee, Dr. N. J. Singh, Prof. K. S. Kim
Center for Superfunctional Materials
Department of Chemistry
Pohang University of Science and Technology
Pohang 790-784 (Korea)
Fax: (+82) 54-279-8137
E-mail: kim@postech.ac.kr

[b] S. W. Heo,[+] Prof. S. B. Kim
Department of Chemistry
Pohang University of Science and Technology
Pohang 790-784 (Korea)

[+] These authors contributed equally to this work.

Supporting information for this article is available on the WWW under http://dx.doi.org/10.1002/asia.201100130.

cationic hydrogen bonds are, in general, slightly shorter than anionic hydrogen bonds.[12,14]

There have been several crystal structures of proton-bonded complexes.[7,8] However, the progress of proton bonds in the solid state has been very limited and a clear assignment of the IR signatures, in particular, for C=O–H$^+$–O=C in the solid state is yet to be made because of the complicated nature in the spectral pattern. In the IR spectra of protonated benzophenone crystals, the broad signals below 2000 cm^{-1} are partly associated with C=O stretching modes and O–H$^+$–O stretching and bending modes and so the exact assignment of IR signals is not possible owing to the overlap of such modes with other modes of the organic molecule. Furthermore, a systematic Cambridge Crystallographic Data Centre (CCDC) search of the O–H$^+$–O proton bonds shows that the crystal structure of proton-bonded aldehydes and polyaromatic hydrocarbon (PAH) compounds are rarely reported in the literature, except for our recent studies of proton arrays.[15] To understand and utilize this special type of cationic hydrogen bond, it is vital to have the relevant crystal structures and spectral signatures of O–H$^+$–O proton bonds. Thus, we have investigated the proton-bonded crystal structure of [(Py-CHO)$_2$H][AuCl$_4$] (**I**).

Results and Discussion

In the proton-bonded crystal structure of **I**,[16] a proton is coordinated linearly with two oxygen atoms of the π-electron-rich PAHs with carbonyl aldehyde functional ligands, 1-pyrenecarbaldehyde (Py-CHO; C_{2h} symmetry). This proton complex has a yellowish orange color as a result of the interaction of Py-CHO with HAuCl$_4$. It is then crystallized into red platelike formic crystals of **I** by slow evaporation of organic solvents (MeOH, EtOH, CHCl$_3$, CH$_3$Cl, CH$_3$CN, etc.). The appearance of the red color in these solid crystals is due to the existence of O–H$^+$–O in the solid state (see the Supporting Information).

The crystal structure of **I** (Figure 1) shows the intermolecular π–π interactions[17] of polyaromatic compounds as well as the proton-bonded aldehyde dimers. The unit cell structure contains one molecule. The crystal structure is constructed of a layer structure along the *b* axis comprising of 2D cationic layers (Py-CHO and proton bond) and counteranion layers of [AuCl$_4$]$^-$ anions (see the Supporting Information). At 100 K, the O···O distance is 2.427(3) Å. In the crystallographic analysis, the bridging proton-like hydrogen atoms are clearly identified with weak electron densities (see the Supporting Information). Each central O–H$^+$–O unit is linear (180°), and the O–H distance is 1.213(3) Å. Owing to proton bonding, the C=O bond length, which is 1.202(4) [18a] or 1.194(5) Å[18b] in crystalline Py-CHO, increases to 1.257(1) Å.

The proton bond may be considered as a special type of hydrogen bond. This terminology was used recently.[9] To address whether the proton bond is distinguishable from the hydrogen bond, it is necessary to investigate the charge of the hydrogen atom involved in the proton/hydrogen bond. At the DFT level using the BLYP functional with the 6-31G* basis set, which we employed herein for the geometric and spectral study of **I** owing to the large molecular size, the natural bond orbital (NBO) charge of the hydrogen atom in **I** was calculated to be 0.51 au, which was in between a proton and a hydrogen atom. This value (or 0.55 au in H$^+$

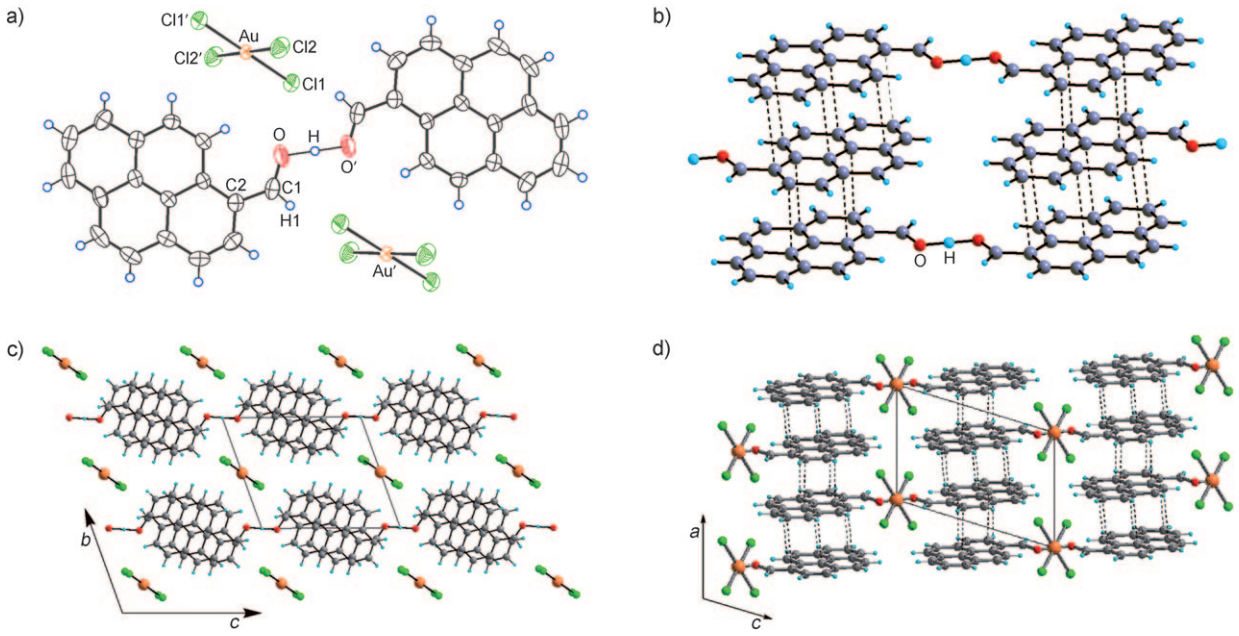

Figure 1. a) An ORTEP representation of the molecular structure of **I** with the triclinic space group $P\bar{1}$. Thermal ellipsoids are shown at the 50% probability level. b) A diamond graphic diagram showing the π–π intermolecular interactions as dotted lines (d(C···C)≈3.38(3) Å) and the proton bond with a distance of d(O···O)=2.427(3) Å) at 100 K.[16] The proton lies on a center of inversion. Projections of the unit cell structure into the *a*,*c* (c) and the *b*,*c* planes (d) are also shown.

$(H_2O)_2$, i.e., $H_5O_2^+$) was compared with the hydrogen atomic charges in the anionic hydrogen bonds (0.45 au in $H^+(OH^-)_2$, i.e., $H_3O_2^-$) and neutral hydrogen bonds (0.46 au in the water dimer $(H_2O)_2$). More reliable NBO charges at the MP2/aug-cc-pVDZ level of theory (0.58 au for $H^+(MeCHO)_2$; 0.60 au for $H^+(H_2O)_2$; 0.51 au for $(H_2O)_2$) indicated that the H^+ atom in $H^+(MeCHO)_2$ and $H^+(H_2O)_2$ was likely to behave like a proton rather than as a hydrogen atom. These protonated species show a clear difference in electron density distribution between the proton bond and normal bond. In the case of the proton bond, the weak electron density of O–H^+–O is more delocalized (showing that the hydrogen atom almost behaves like a proton because most of the electron density is distributed toward to the two oxygen atoms) than the strong electron density in O–H–O. The electron density of the hydrogen atom in O–H^+–O is diffused toward the oxygen atoms with the formation of the strong H^+–O bond (Figure 2). However, in the case of the normal hydrogen bond the electron density of the hydrogen atom is almost localized around the hydrogen nucleus (hence less positively charged). Thus, compared with the neutral hydrogen or anionic hydrogen bond, the positively charged hydrogen bond has a more positively charged value for the hydrogen atom between the two oxygen atoms, thus showing more proton-bond characteristics. Furthermore, the O–H^+–O frequencies around 700–1000 cm^{-1} are quite different from the O···H bond-stretching signal ($\approx$200 cm^{-1}) and the O–H stretching signal ($\approx$3000–3700 cm^{-1}) in a normal hydrogen bond.[6,9] Hence, this O–H^+–O bond is considered to be a proton bond, rather than a hydrogen bond, as evidenced from its unusual characteristics in the IR spectral signature.

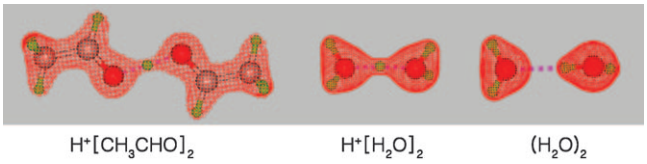

Figure 2. A comparison of electron densities of protonated hydrogen bonds and normal hydrogen bonds.

Most molecular packing systems of PAH derivatives are constructed in a herringbone-type arrangement with intermolecular polyaromatic interactions composed of π–π and H–π[19] interactions. For example, pyrene molecules have two structural forms: 1) the sandwich–herringbone structure with H–π interactions between the dimers, each of which is composed of two parallel stacks at normal pressure and 2) the high-pressure polymorph with graphite-like π–π stacking (vertical distance $\approx$3.4 Å and an off-center ring displacement of $\approx$1.6 Å.) at high-pressure (0.3–0.5 GPa).[20] In the case of 1Py-CHO crystals, the vertical distance is 3.44 Å with an off-center displacement of 1.61 Å between the two rings.[21] However, the structure-packing systems of the proton complex **I** show only graphite-like π–π stacking with slightly shorter vertical π-stacking distances than in the cases of pyrene and Py-CHOs. The vertical distance and off-center ring displacement of the π–π stacking are 3.378 Å and 1.55 Å, respectively, for the pyrene moieties in **I**. The square-planar structure of $[AuCl_4]^-$ counteranions is stabilized with linear intermolecular hydrogen bonds (C(=O)–H···Cl; d(H···Cl) = 2.738 Å). They are lined up along the a axis and constructed in an ionic salt layer along the b axis.

The temperature dependence of the physical properties of a single crystal of **I** was investigated at various temperatures (from 100 to 370 K) by synchrotron X-ray crystallography at the Pohang Accelerator Laboratory (PAL),[16] differential scanning calorimetry (DSC), and FTIR spectroscopy. The temperature-dependence parameters are summarized in Figure 3 a–d. As the temperature increases from 100 to 300 K, the distance between the two oxygen atoms in the O–H^+–O

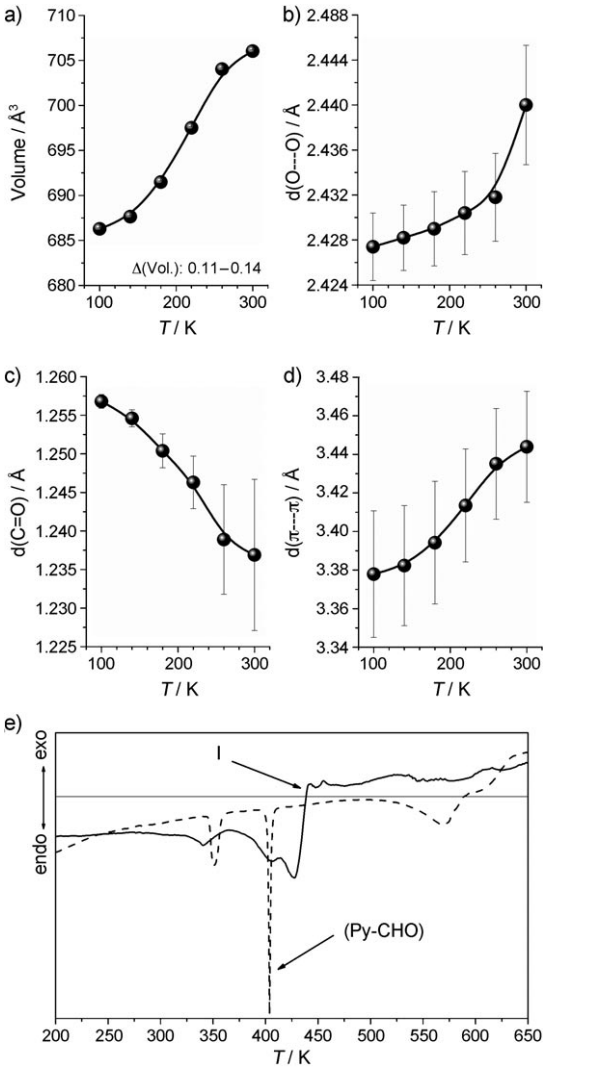

Figure 3. Temperature dependence of the synchrotron X-ray crystal structure of **I** on a) the lattice volume, b) the O–(H^+)–O distance, c) the C=O distance, and d) the vertical π-stacking distance in the temperature range 100–300 K. e) DSC analysis of **I** compared with that of Py-CHO (dashed line). The temperature was increased by 10 K min^{-1} in the range 190–700 K.

moiety increases by 0.013 Å, the C=O distance decreases by 0.02 Å, and the vertical π-stacking distances of pyrene moieties increase by 0.066 Å.

The temperature-dependent distance changes are clear with much larger values than the error ranges. There are no significant phase changes below 300 K. As the temperature increases, the increase in the O–H^+–O distance is expected owing to the slightly weakened proton bond. The increase in the O–H^+–O distance would not be significantly affected by the π–π stacking distance change because the π–π interaction is weak. This increase in O–H^+–O distance with increasing temperature is consistent with the increase in O–H–N distance in the heteronuclear hydrogen bonds of adducts of pentachlorophenol with pyridine, which were studied by variable-temperature time-of-flight Laue neutron diffraction analysis.[22]

Thermal structural transformations have been studied by DSC in the temperature range 190–700 K (Figure 3e). The proton-bonded complex **I** undergoes a gradual endo- to exothermic transition at 427 K as it decomposes. Its thermal stability is considerably enhanced relative to that (404 K) of Py-CHO. Over the decomposition temperature (423 K), the red compound changed to black with the formation of black charred material composed of gold particles in graphene[23] films, that is, graphene-like material and gold–graphene hybrid material. Thus, this would be one possible method to make metal–graphene hybrid materials.[24]

The IR spectra of KBr pellets (500 to 4000 cm^{-1} range) of the red platelike crystals were recorded every 10 K in the temperature range from 123 to 423 K (selected spectra are shown in Figure 4a). The temperature-dependent IR spectra of **I** are compared with the room-temperature IR spectra of Py-CHO. The IR spectra of **I** below the decomposition temperature show an interesting change in the signal pattern compared with that of Py-CHO. The vibration modes ν(C=O) and ν(C–H), marked with an asterisk (1680/1668 and 2714/2770, 2855 cm^{-1}), for the aldehyde groups of Py-CHO disappear in **I** owing to the formation of proton complexes. As for the new absorption vibration modes of the O–H^+–O moiety in FTIR spectra of both proton complexes, we assign the stretching and the bending mode as ν_{as}(851, 905 cm^{-1}) and δ(1662 cm^{-1}) for **I** at 123 K. This assignment was made by comparing spectral changes upon increasing the temperature from 123 to 393 K and the theoretically calculated IR spectra of these compounds using DFT (BLYP/6-31G*) (Table 1).

We have previously noted that the calculated harmonic/anharmonic vibrational frequencies (at the BLYP/aug-cc-pVDZ level of theory) of stretching (≈974/983 cm^{-1}) and bending (≈1693/1702 cm^{-1}) modes for the classical example of the Zundel ion cluster of O–H^+–O in $H_5O_2^+$ tended to be underestimated with respect to the corresponding gas-phase experimental IR values of about 1000 and

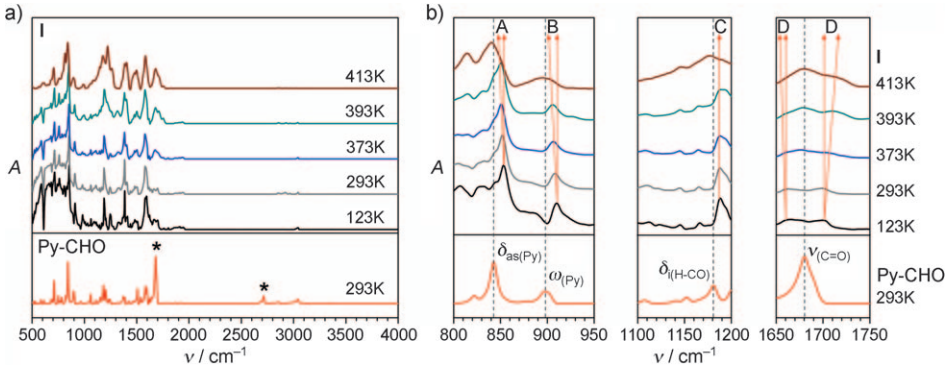

Figure 4. a) IR spectra of **I** at selected temperatures (123–413 K). b) Expansion of selected frequency ranges of the (O–H–O) mode. At 293 K, the characteristic frequencies of Py-CHO are at 843 (Py ring distortion), 898 (ω(Py)), 1181 (δ_i(CH) of Py), and 1680 cm^{-1} (ν(C=O) of CHO). At temperatures between 123 and 393 K, the characteristic frequencies of **I** appear at around 853 (A) and 910 (B) (ν(O–H^+–O)), at 1188 (C) (δ_o(OHO)), and at 1665 and 1700 cm^{-1} (D) (δ_i(OH^+O)) (ν: stretching, δ_i: in-plane bending, δ_o: out-of-plane bending, ω: wagging). Around 403–413 K, these signals disappear and the Py-CHO signals reappear, indicating breaking of the proton-bonded dimer into monomers.

Table 1. Selected experimental IR absorption peaks (frequencies in cm^{-1}) for **I** (at 123–413 K) and Py-CHO (at room temperature) along with the predicted frequencies at the BLYP/6-31G* level of theory.[a]

	Exptl				Calcd	Mode
	123 K	293 K	393 K	413 K		
		843			844(8)	ω(Py)
		898			881(4)	Py ring distortion
Py-CHO		1181			1184(7)[b]	δ_i(CH) of Py
		1680			1663(25)	ν(C=O) of CHO
		2714			2712(23)	ν(C-H) of CHO
	844	844	844	841	846(10)	ω(Py)
	nv	nv	nv	896	892(85)[b]	Py ring distortion
	853	852	851	–	867(1112)	ν(O–H) of OHO
	910	908	905	–	906(675)	
	1188	1187	1189	–	1145(6)	δ_o(OHO)
I	nv	nv	nv	1178	1175(7)[b]	δ_i(CH) of Py
	1665	1662	–	–	1603(17)	δ_i(OHO)
	1700	1699			1646(9)	
	–	–	1680	1680	–	ν(C=O) of CHO
	2848	nv	nv	nv	2877(6)	ν(C-H) of CHO
	2916				2926(3)	

[a] BLYP/6-31G* frequencies (f^i) are scaled (f^s) exponentially with $\alpha = 0.92961 \times 10^{-5}$ [$f^s = f^i \exp(-\alpha f^i)$].[25] The values in parentheses are the IR intensity at 10 km mol^{-1}. nv: not visible. [b] This band would be invisible owing to the very strong O–H–O stretching bands at 867 and 906 cm^{-1}.

1800 cm^{-1}.[6] However, with the increasing number of water molecules in $H_5O_2^+(H_2O)_4$, we see an improvement to 985 cm^{-1} (anharmonic: 994 cm^{-1})[6] in the calculated harmonic vibrational frequency of the stretching mode of O–H^+–O. In **I** in which both sides of the O–H^+–O moiety are substituted with large organic moieties, the calculated harmonic frequencies reproduce the solid-state experimental IR values reasonably well. The vibrational bands of **I** at 293 K are assigned for stretching ν(OH) at 852 and 908 cm^{-1}, out-of-plane OHO bending δ_o(OHO) at 1188 cm^{-1}, and in-plane OHO bending δ_i(OHO) at 1662 and 1699 cm^{-1}, in comparison with the calculated values for ν(OH) of 867 and 906 cm^{-1}, δ_o(OHO) of 1145 cm^{-1}, and δ_i-(OHO) of 1603 and 1646 cm^{-1}. The broad bands below 850 cm^{-1} are due to the activation of several vibrational modes, such as wagging and in-/out-of-plane ring distortion of the pyrene rings in **I**. The ν(C=O) signal (1680 cm^{-1}) of Py-CHO is not visible in **I** between 123 and 393 K, whereas the ν(C–H) signal (2714 cm^{-1}) of Py-CHO shifts to 2848 and 2916 cm^{-1} at 123 K. The ν(C–H) signals of CHO groups of **I** are not visible at high temperatures. The disappearance and shift in the IR signal positions for the vibrational modes of CHO in **I** is due to the formation of the OH^+O bond between two Py-CHO monomers. However, above 393 K, the ν(C=O) band starts appearing at 1680 cm^{-1} and the δ_i-(OHO) bands start losing their identity. At 413 K, the ν(C=O) signal is the dominant one in this region. Temperature-dependent IR spectral analysis of **I** clearly suggests the existence of a stable OH^+O moiety up to around 383 K, the start of OH^+O bond breaking at 393 K, and the complete dissociation of proton bonds at 413 K. It is particularly interesting to note that the OH^+O bond is stabilized up to around 390 K.

The red crystals are very stable under dry conditions at room temperature for a long time and the color of the crystal remains unchanged. In various solvents (H_2O, alcohol, CH_3CN, etc.), they are dissociated into a yellow solution of $HAuCl_4$ and a yellow suspension of pyrenealdehyde. However, dilution ($<10^{-3}$ mmol) gives a light-orange color. The PAH aldehyde ligands could also be used for the protonation reaction with anhydrous sulfuric acid (98%) in dichloromethane.[26] Additionally, a UV/Vis spectroscopic study of the red crystalline particles and anhydrous red liquid state gives no differential signals of absorption bands. Upon dilution of the red liquid state, the color of the solution turns back to yellow as a result of the deprotonation of **I**, hence the absorption spectra of **I** (protonated form) in solution cannot be recorded. The change in color from yellow to red upon complex formation is due to a small charge transfer from the aromatic ring to the O–H^+–O moiety from theoretical calculations.[16] The protonation of Py-CHO leads to the extended delocalization of the π electrons, including the C(1)–CHO bond associated with the decrease in the bond length from 1.48 Å in Py-CHO to 1.39 Å in Py-CHO–H^+. This extended delocalization of the π electrons results in lowering the band gap in Py-CHO–H^+, that is, changing from yellow to red in color. In the presence of water, the color turns from red to yellow because charge transfer is not possible as the proton reacts with water molecules. Because this change is very sensitive, the crystal can be utilized as a moisture sensor.

Conclusion

We have reported the first intermolecular proton-bonded aldehydes of a PAH system. The charge of the hydrogen involved in the O–H^+–O bond is 0.51 au (at BLYP/6-31G*) or 0.58 au (at MP2/aug-cc-pVDZ), suggesting that the hydrogen is somewhat proton-like. The color change from yellow to red upon proton complex formation was due to a small charge transfer from the aromatic ring to the O–H^+–O moiety, which resulted in lowering the band gap by the extended delocalization of the π electrons.

Thermal structural transformations were investigated by FTIR spectroscopy, DSC, and synchrotron X-rays. The π stacking became disordered at 393 K and the proton bonds broke at 403 K. Owing to the π–π interactions, the proton-bonded system was stabilized up to 393 K.

At temperatures ranging from 123 to 423 K, the Zundel-like proton signature (showing that the proton was in the middle of two O atoms at a distance of only ≈2.4 Å) from the O–H^+–O vibrational spectra has been investigated down to 500 cm^{-1}, which was much lower than the lowest frequency of gas-phase IR spectroscopy experiments reported so far. These low frequencies were very clear in the crystals. The characteristic signals of the O–H^+–O vibrational spectra were 850 and 909 cm^{-1} for the stretching modes and 1621 and 1670 cm^{-1} for the bending modes. Clear observation of characteristic signals of O–H^+–O in the low-frequency ranges in the solid state undoubtedly aided better understanding of the complexes composed of O–H^+–O moieties in both gas and condensed phases.

As the temperature increased from 100 to 300 K, the O–H^+–O distance increased by 0.013 Å, and the vertical π-stacking distances increased by 0.066 Å.

Experimental Section

Compound **I** was prepared by the reaction of $HAuCl_4$·3(H_2O) (170 mg, 0.431 mmol) and Py-CHO (200 mg, 0.869 mmol) in CH_3CN/CH_3Cl (or CH_3CN/CH_2Cl_2) at 20 °C. The purple platelike crystals were obtained in an inert gas system (argon or nitrogen) by the slow evaporation of solvents at room temperature for 3 days. After isolation, the product was characterized by X-ray single-crystal structure analysis and IR spectroscopy. ^{1}H NMR (500 MHz, $CDCl_3$) spectra obtained were those of the reactant of 9-pyrenecarbaldehyde after dissociation in organic solvents. IR (RT, solid): $\tilde{\nu}$ = 3045(10), 1950–1740 (br weak), 1670(30), 1587(45), 1508(25), 1385(30), 1246(25), 1188(35), 1063(6), 910(25), 852(100) cm^{-1}; MALDI-TOF MS: *m*/*z*: 231 [($C_{18}H_{10}O$)+H^+], 339 [$AuCl_4^-$].

Crystal Structure Analysis

A crystal of **I** was measured on a Bruker-SMART-AFEX-diffractometer (λ = 0.71073 Å)[18b] and an ADSC Quantum 210 CCD diffractometer with synchrotron radiation (λ = 0.80000 Å) at the Macromolecular Crystallography Wiggler Beamline 4A, Pohang Accelerator Laboratory.[16] By using

the latter, the low-temperature diffraction data from a single crystal of **I** ($0.10\times0.05\times0.05$ mm^3) were collected from 100 to 333 K. The crystal was rotated through 360°. The raw data were processed and scaled by using the program HKL2000.[27] The structure was solved by direct methods and the refinements were carried out with full-matrix least-squares on F^2 by using the Bruker SHELXTL program package.[28] All atoms were refined anisotropically. The temperature dependence for the proton-binding properties of the single crystals was investigated at various temperatures (from 100 to 370 K) with synchrotron X-ray crystallography.

CCDC 660015 ($[H(C_{18}H_{10}O)_2]^+[AuCl_4]^-$) contains the supplementary crystallographic data for this paper. These data can be obtained free of charge from the Cambridge Crystallographic Data Centre via www.ccdc.cam.ac.uk/data_request/cif.[16]

FTIR Spectra

FTIR spectra were measured at a spectral resolution of 4 cm^{-1} with a Bruker IFS 66v/S FTIR spectrometer equipped with a liquid-nitrogen-cooled mercury cadmium telluride (MCT) detector. The samples were studied as powders dispersed in a KBr pellet. Variable-temperature spectra were measured with an AABSPEC 2000 multimode experimental chamber. All FTIR spectra were measured by co-adding 256 scans. The sample and source compartments were evacuated to 1 mbar. FTIR spectra of KBr pellets (500 to 4000 cm^{-1} range) of the red platelike crystals were recorded every 10 K in the temperature range from 123 to 423 K

DSC Analysis

DSC thermograms were measured under a nitrogen atmosphere over the temperature range 173–673 K by using a calorimeter (model DSC-220CU, Seiko instruments) calibrated with indium and tin standards. The heating and cooling rates were 10.0 K min^{-1}.

Acknowledgements

This work was supported by the NRF (National Honor Scientist Program: 2010-0020414, WCU:R32-2008-000-10180-0) and BK21. Most calculations were carried out by using supercomputers at KISTI (grant no. KSC-2008K08-0002). The temperature-dependent X-ray characterization was carried out by using the synchrotron source at PAL (Beamline 4A, 6B; 2010-1063-18).

[1] *Hydrogen Bonding-New Insights* (Ed.: S. J. Grabowski), Springer, Dordrecht, **2006**.

[2] C. Pak, H. M. Lee, J. C. Kim, D. Kim, K. S. Kim, *Struct. Chem.* **2005**, *16*, 187–202.

[3] a) N. J. Singh, H. M. Lee, I.-C. Hwang, K. S. Kim, *Supramol. Chem.* **2007**, *19*, 321–332; b) H. Ihm, S. Yun, H. G. Kim, J. K. Kim, K. S. Kim, *Org. Lett.* **2002**, *4*, 2897–2900; c) J. D. Dunitz, A. Gavezzotti, *Angew. Chem.* **2005**, *117*, 1796–1819; *Angew. Chem. Int. Ed.* **2005**, *44*, 1766–1787; d) S. Odde, B. J. Mhin, S. Lee, K. S. Kim, *J. Chem. Phys.* **2004**, *120*, 9524–9535.

[4] a) H. M. Lee, S. B. Suh, J. Y. Lee, P. Tarakeshwar, K. S. Kim, *J. Chem. Phys.* **2000**, *112*, 9759–9772; b) J. Kim, K. S. Kim, *J. Chem. Phys.* **1998**, *109*, 5886–5895.

[5] a) W. W. Cleland, M. M. Kreevoy, *Science* **1994**, *264*, 1887; b) K. S. Kim, D. Kim, J. Y. Lee, P. Tarakeshwar, K. S. Oh, *Biochemistry* **2002**, *41*, 5300; c) P. A. Frey, S. A. Whitt, J. B. Tobin, *Science* **1994**, *264*, 1927–1930; d) K. S. Kim, K. S. Oh, J. Y. Lee, *Proc. Natl. Acad. Sci. USA* **2000**, *97*, 6373–6378.

[6] a) J. M. Headrick, E. G. Diken, R. S. Walters, N. I. Hammer, R. A. Christie, J. Cui, E. M. Myshakin, M. A. Duncan, M. A. Johnson, K. D. Jordan, *Science* **2005**, *308*, 1765–1769; b) N. J. Singh, M. Park, S. K. Min, S. B. Suh, K. S. Kim, *Angew. Chem.* **2006**, *118*, 3879–3884; *Angew. Chem. Int. Ed.* **2006**, *45*, 3795–3800; c) M. Miyazaki, A. Fujii, T. Ebata, N. Mikami, *Science* **2004**, *304*, 1134–1137; d) J. W. Shin, N. I. Hammer, E. G. Diken, M. A. Johnson, R. S. Walters, T. D. Jaeger, M. A. Duncan, R. A. Christie, K. D. Jordan, *Science* **2004**, *304*, 1137–1140; e) K. N. Asmis, N. L. Pivonka, G. Santambrogio, M. Brummer, C. Kaposta, D. M. Neumark, L. Woste, *Science* **2003**, *299*, 1375–1377.

[7] a) C. L. Perrin, J. B. Nielson, *Annu. Rev. Phys. Chem.* **1997**, *48*, 511–544; b) D. Madsen, C. Flensburg, S. Larsen, *J. Phys. Chem. A* **1998**, *102*, 2177–2188; c) P. Gilli, V. Bertolasi, L. Pretto, V. Ferretti, G. Gilli, *J. Am. Chem. Soc.* **2004**, *126*, 3845–3855.

[8] a) C. L. Hill, D. A. Bouchard, M. Kadkhodayan, M. M. Williamson, J. A. Schmidt, E. F. Hilinski, *J. Am. Chem. Soc.* **1988**, *110*, 5471–5479; b) E. F. Kleinman, J. Bordner, B. J. Newhouse, K. MacFerrin, *J. Am. Chem. Soc.* **1992**, *114*, 4945; c) M. W. Esterhuysen, H. G. Raubenheimer, *Eur. J. Inorg. Chem.* **2003**, 3861–3869.

[9] J. R. Roscioli, L. R. McCunn, M. A. Johnson, *Science* **2007**, *316*, 249–254.

[10] a) S. B. Suh, J. C. Kim, Y. C. Choi, K. S. Kim, *J. Am. Chem. Soc.* **2004**, *126*, 2186–2193; b) N. Kobko, L. Paraskevas, E. del Rio, J. J. Dannenberg, *J. Am. Chem. Soc.* **2001**, *123*, 4348–4349.

[11] B. H. Hong, J. Y. Lee, C.-W. Lee, J. C. Kim, S. C. Bae, K. S. Kim, *J. Am. Chem. Soc.* **2001**, *123*, 10748–10749.

[12] H. M. Lee, A. Kumar, M. Kolaski, D. Y. Kim, E. C. Lee, S. K. Min, M. Park, Y. C. Choi, and K. S. Kim, *Phys. Chem. Chem. Phys.* **2010**, *12*, 6278–6287.

[13] M. Park, I. Shin, N. J. Singh, K. S. Kim, *J. Phys. Chem. A* **2007**, *111*, 10692–10702.

[14] a) M. Kołaski, A. Kumar, N. J. Singh and K. S. Kim, *Phys. Chem. Chem. Phys.* **2011**, *13*, 991–1001; b) K. S. Oh, C. W. Lee, H. S. Choi, S. J. Lee, K. S. Kim, *Org. Lett.* **2000**, *2*, 2679–2681.

[15] I.-C. Hwang, S. W. Heo, N. J. Singh, J. W. Lee, Y. Chun, S. B. Baek, K. S. Jin, M. Ree, H. C. Lee, S. B. Kim, and K. S. Kim, *J. Phys. Chem. B* **2010**, *114*, 7216–7221.

[16] The low-temperature diffraction data from a single crystal of **I** ($0.10\times0.05\times0.05$ mm^3) were collected from 100 to 333 K on a ADSC Quantum 210 CCD diffractometer with synchrotron radiation ($\lambda=0.8000$ Å) at the Macromolecular Crystallography Wiggler Beamline 4A, Pohang Accelerator Laboratory. $C_{34}H_{21}O_2AuCl_4$; $M_r=800.27$ Å^3; triclinic; $P\bar{1}$ (no. 2); $a=7.520(1)$, $b=9.211(1)$, $c=11.122(1)$ Å; $\alpha=106.600(2)$, $\beta=102.552(2)$, $\gamma=100.740(1)$°; $V=694.75(13)$ Å^3; $Z=1$; $T=100$ K; GOF = 1.234; $R_1(I>2\sigma(I))=0.0439$, $wR_2=0.1394$. Crystallographic data for **I** obtained by using a Bruker SMART AFEX diffractometer ($\lambda=0.71073$ Å): $C_{34}H_{21}O_2AuCl_4$; $M=800.27$ Å^3; triclinic; $P\bar{1}$ (no. 2); $a=7.5499(6)$, $b=9.2759(8)$, $c=11.1030(9)$ Å; $\alpha=106.353(1)$, $\beta=103.084(1)$, $\gamma=100.209(2)$°; $V=702.17(10)$ Å^3, $Z=1$; $T=243$ K; GOF = 1.037: $R_1(I>2\sigma(I))=0.0314$, $wR_2=0.0338$.

[17] a) K. S. Kim, P. Tarakeshwar, J. Y. Lee, *Chem. Rev.* **2000**, *100*, 4145–4185; b) E. C. Lee, D. Kim, P. Jurečka, P. Tarakeshwar, P. Hobza, and K. S. Kim, *J. Phys. Chem. A* **2007**, *111*, 3446–3457; c) N. J. Singh, S. K. Min, D. Y. Kim, and K. S. Kim, *J. Chem. Theory Comput.* **2009**, *5*, 515–529.

[18] a) S. Y. Matsuzaki, M. Goto, K. Honda, I. Kojima, *Anal. Sci.* **1995**, *11*, 461–463; b) A. Camerman, J. Trotter, *Acta Crystallogr.* **1965**, *18*, 636–643.

[19] a) E. C. Lee, B. H. Hong, J. Y. Lee, J. C. Kim, D. Kim, Y. Kim, P. Tarakeshwar, K. S. Kim, *J. Am. Chem. Soc.* **2005**, *127*, 4530–4537; b) P. Tarakeshwar, H. S. Choi, K. S. Kim, *J. Am. Chem. Soc.* **2001**, *123*, 3323–3331; c) P. Tarakeshwar, S. J. Lee, J. Y. Lee, K. S. Kim, *J. Phys. Chem.* **1998**, *108*, 7217–7223.

[20] a) F. P. A. Fabbiani, D. R. Allan, S. Parsons, C. R. Pulham, *Acta Crystallogr. Sect. B* **2006**, *62*, 826–842; b) G. R. Desiraju, A. Gavezzotti, *Acta Crystallogr. Sect. B* **1989**, *45*, 473–482.

[21] S. Y. Matsuzaki, M. Goto, K. Honda, I. Kojima, *Anal. Sci.* **1995**, *11*, 461–463.

[22] T. Steiner, I. Majerz, C. C. Wilson, *Angew. Chem.* **2001**, *113*, 2728–2731; *Angew. Chem. Int. Ed.* **2001**, *40*, 2651–2654.

[23] a) K. S. Kim, Y. Zhao, H. Jang, S. Y. Lee, J. M. Kim, K. S. Kim, J.-H. Ahn, P. Kim, J.-Y. Choi, B. H. Hong, *Nature* **2009**, *457*, 706–710; b) S. Bae, H. Kim, Y. Lee, X. Xu, J.-S. Park, Y. Zheng, J. Balakrishnan, T. Lei, H. R. Kim, Y. I. Song, Y.-J. Kim, K. S. Kim, B. Ozyilmaz,

J.-H. Ahn, B. H. Hong, S. Iijima, *Nat. Nanotechnol.* **2010**, *5*, 574–578.

[24] a) V. Chandra, J. Park, Y. Chun, J. W. Lee, I.-C. Hwang, K. S. Kim, *ACS Nano* **2010**, *4*, 3979–3986; b) V. Chandra, K. S. Kim, *Chem. Commun.* **2011**, *47*, 3942–3944.

[25] a) J. Y. Lee, O. Hahn, S. J. Lee, H. S. Choi, B. J. Mhin, M. S. Lee, K. S. Kim, *J. Phys. Chem.* **1995**, *99*, 2262–2266; b) J. Y. Lee, O. Hahn, S. J. Lee, H. S. Choi, H. S. Shim, B. J. Mhin, K. S. Kim, *J. Phys. Chem.* **1995**, *99*, 1913–1918.

[26] A. U. Acuña, J. M. Otón, *J. Lumin.* **1979**, *20*, 379–385.

[27] Z. Otwinowski, W. Minor in *Methods in Enzymology*, Vol. 276, *Macromolecular Crystallography, Part A* (Eds.: C. W. Caret, Jr., R. M. Sweet), **1997**, pp. 307–326.

[28] a) G. Sheldrick, *Program for Crystal Structure Solution*, Universität Göttingen, Göttingen (Germany), **1986**; b) G. Sheldrick, *Program for Crystal Structure Refinement*, Universität Göttingen, Göttingen (Germany), **1993**.

Received: February 9, 2011
Published online: May 27, 2011

